

Prolate-oblate problem in ^{28}Si : Angular-momentum projection before and after variation

W. Bauhoff

*I. Institut für Experimentalphysik, Universität Hamburg,
D-2000 Hamburg 50, West Germany*

H. Schultheis and R. Schultheis

*Institut für Theoretische Physik, Universität Tübingen,
D-7400 Tübingen, West Germany*

(Received 22 March 1982)

The effect of angular momentum and parity projection on the energy and deformation of the oblate and prolate minimum in ^{28}Si has been studied. We discuss the approximations resulting from variation without, before, and after projection for a number of standard nucleon-nucleon interactions. We find that the intrinsic oblate and prolate minimum occur in reversed energetical order for most forces. The effect of angular momentum projection alone tends to resolve the discrepancy but this effect is reduced if the projected states are allowed to vary.

[NUCLEAR STRUCTURE ^{28}Si ; alpha-cluster model variation after
projection with finite-range forces. Calculated energies, quadrupole mo-
ments, rms radii.]

I. INTRODUCTION

The coexistence of an oblate ground state and an excited prolate minimum in ^{28}Si has been a challenge for a large number of nuclear structure calculations using such diverse methods as Hartree-Fock,¹⁻¹⁷ Hartree-Fock-Bogoliubov,^{18,19} shell model,^{20,21} SU(3),^{22,23} the Strutinsky correction,^{24,25} generator coordinate,^{26,27} and alpha-cluster model approaches.²⁸⁻³¹

Experimentally, the first three 0^+ levels³² in ^{28}Si are the ground state with negative quadrupole moment, a 4.979 MeV level that has been attributed¹ to a vibrational excitation in the oblate well, and the 6.691 MeV band head of a prolate band that has recently been identified.³³ While many theoretical studies confirm the existence of two local minima with prolate and oblate deformation, most calculations fail to reproduce the energy spacing of the corresponding experimental levels. Although the observed 6.691 MeV excitation of the prolate state is quite large, the calculated prolate and oblate minima tend to be almost degenerate in many cases or occur even in reversed order.

The present paper deals with the effect of angular momentum projection on the oblate and prolate minimum in ^{28}Si . Many previous calculations in

^{28}Si are for the intrinsic states only (Refs. 1, 3-6, 11-13, 16-19, 24, 25, and 28-30), and do not take into account states of good angular momentum. It has been speculated that angular momentum projection might remedy the unsatisfactory level sequence obtained for the intrinsic states. In fact, an improvement has been found in some cases (Refs. 8, 10, and 15), where angular momentum projection was applied to the intrinsic minimum-energy states (i.e., after variation). However, with few exceptions,^{7,9,27,31} no attempt has been made to study if the improvement obtained by angular momentum projection (without further variation) persists under the complete variation of the projected states. For the Brink-Boeker B_1 interaction,³⁴ it has been found³¹ that the relative effect of the projection in the oblate and prolate state of ^{28}Si is reversed if the projected state is allowed to vary.

We have studied the results of angular momentum projection in ^{28}Si for a number of standard nucleon-nucleon interactions and allowed for deviations from axial symmetry in the intrinsic state. In the following we present the results of the usual approximations, viz., variation without, before, and after projection, and discuss the improvement or deterioration obtained from the consecutive approximations.

II. METHOD

A. Intrinsic states

Throughout this paper Brink's alpha-cluster model (ACM) wave functions³⁵ are used as the intrinsic variational many-body states of the nucleus, i.e., Slater determinants $|\Phi\rangle$ of (in general nonorthogonal) $1s$ harmonic-oscillator single-nucleon orbitals with quartet coupling that are centered around given positions \vec{R}_j ,

$$\phi_i(\vec{x}_i) = (b/\sqrt{\pi})^{-3/2} \exp[-(\vec{x}_i - \vec{R}_j)^2/2b^2] \chi_i \quad (i=1, \dots, A; j=1, \dots, A/4). \quad (2.1)$$

In Eq. (2.1) i labels the nucleons and j the alpha centers, χ_i denotes the spin and isospin state of the nucleon, and b is the oscillator width.

The choice of this type of variational many-body state is motivated by the following reasons: Firstly, no Lagrange constraint is needed to search for a local energy minimum that is well enough separated from the absolute minimum of the variational space. This property is particularly useful for this study as the ambiguities associated with the choice of one or several constraints can be avoided. Secondly, the numerical angular momentum projection of nonaxial intrinsic states is still practical although explicit K projection and, therefore, a three-fold rather than single quadrature, are required in the Peierls-Yoccoz projection integral (cf. Sec. II C).

B. Hamiltonian

The calculations have been performed for a number of different finite-range forces of the Brink-Boeker (B and C) and Volkov (V) soft-core type.^{34,36} In any case the exact Coulomb energy and the complete (one- and two-body) center-of-mass term have been included.

The present computation of the matrix elements of the intrinsic states follows standard methods. We refer therefore, e.g., to Refs. 35 and 37 where the explicit form of the matrix elements and more details of ACM calculations are also given.

C. Parity and angular momentum projection

As the intrinsic state $|\Phi(\vec{x}_i, \vec{R}_j, b)\rangle$ of the 28-particle system is determined by the cluster centers $\vec{R}_1, \dots, \vec{R}_7$ (and the oscillator constant b) any reflection or rotation \mathcal{R} of the wave function can be achieved by operating on the parameters \vec{R}_j ($j=1, \dots, A/4$) rather than the particle coordinates \vec{x}_i ($i=1, \dots, A$)

$$|\Phi(-\vec{x}_i; \vec{R}_j, b)\rangle = |\Phi(\vec{x}_i; -\vec{R}_j, b)\rangle, \quad (2.2a)$$

$$|\Phi(\mathcal{R}\vec{x}_i; \vec{R}_j, b)\rangle = |\Phi(\vec{x}_i; \mathcal{R}^{-1}\vec{R}_j, b)\rangle. \quad (2.2b)$$

This facilitates the numerical parity and angular-momentum projection

$$|\Phi^+(\vec{x}_i; \vec{R}_j, b)\rangle = |\Phi(\vec{x}_i; \vec{R}_j, b)\rangle + |\Phi(\vec{x}_i; -\vec{R}_j, b)\rangle \quad \text{and} \quad (2.3)$$

$$P_{KM}^{J+} |\Phi(\vec{x}_i; \vec{R}_j, b)\rangle = \frac{2J+1}{8\pi^2} \int_0^\pi d\beta \sin\beta d_{KM}^J(\beta) \int_0^{2\pi} d\alpha \int_0^{2\pi} d\gamma e^{i(M\alpha + K\gamma)} |\Phi^+(\vec{x}_i; \mathcal{R}_3(\alpha)\mathcal{R}_2(\beta)\mathcal{R}_3(\gamma)\vec{R}_j, b)\rangle. \quad (2.4)$$

In the Peierls-Yoccoz integral (2.4) \mathcal{R} denotes the rotations through the Euler angles α , β , and γ , and d_{KM}^J is the reduced rotation function. The variational ACM states $|\Phi\rangle$, however, are in general nonaxial and require explicit K projections, and therefore numerical integrations over all three Euler angles (α, β, γ).

D. Point symmetry restrictions

The general ACM state of ^{28}Si has 16 variational parameters, viz., the $A/4=7$ cluster positions \vec{R}_j with three coordinates each plus the oscillator constant b , minus the three center-of-mass coordinates,

and to the three Euler angles for the orientation of the system. It is customary in ACM calculations to restrict the variational space to those ACM states that have a given point symmetry. This restriction largely reduces the number of variational parameters but it may lead to spurious results as we showed earlier.^{30,31,38} In contrast to the usual procedure we have first performed an unrestricted 16-parameter variation of the intrinsic state, and then restricted the time-consuming variations after parity and angular momentum projection to the point symmetries that result from the variation without projection, i.e., D_{5h} for the oblate and D_{3h} for the prolate state.

III. RESULTS

The following types of calculations have been performed for a number of nucleon-nucleon forces:

(V): variation of the intrinsic state $|\Phi\rangle$ without projection;

(P^+V): parity projection P^+ of the state $|\Phi\rangle_{\min}$ that results from the unprojected variation (V);

(VP^+): variation of the parity projected state $P^+|\Phi\rangle$;

($P^{0+}V$): parity P^+ and angular momentum projection onto $J=0$ and $K=0$ for $|\Phi\rangle_{\min}$, the result of (V);

(VP^{0+}): variation after projection onto parity + 1, angular momentum $J=0$ and $K=0$.

In addition, projections onto ($J^\pi=2^+$, $K=0$) have been performed for the intrinsic oblate and prolate states, that result from the VP^{0+} calculation, in order to determine the rotational constants of the oblate and prolate bands.

A. Energy shifts and level spacings

Figure 1 shows the energy shifts in the prolate and oblate minima that are associated with the above consecutive approximations for the B_1 force. In any approximation we find two distinct local minima. The intrinsic prolate state has almost good parity. Therefore parity projection has almost no effect on the energy but variation after parity projection leads to a sizable effect. The opposite tendency occurs for the oblate minimum: While a considerable decrease in energy results from the parity projection of the intrinsic minimum, an additional variation leaves this state essentially unaffected. As a result, the variation after parity projection leads to a further decrease of the prolate minimum over the oblate one, and therefore an even larger discrepancy between calculation and experiment. By far the largest effect among all approximations is due to the angular momentum projection. It lowers the oblate minimum about three times as much as the prolate minimum, and reverses the original sequence of the prolate and oblate level, a result that is in accord with the experimental level sequence. A further variation of the parity and angular momentum projected states, however, has the opposite effect: The prolate minimum is lowered four times as much as the oblate one. Among the consecutive approximations this is the largest of all relative shifts in energy between the oblate and pro-

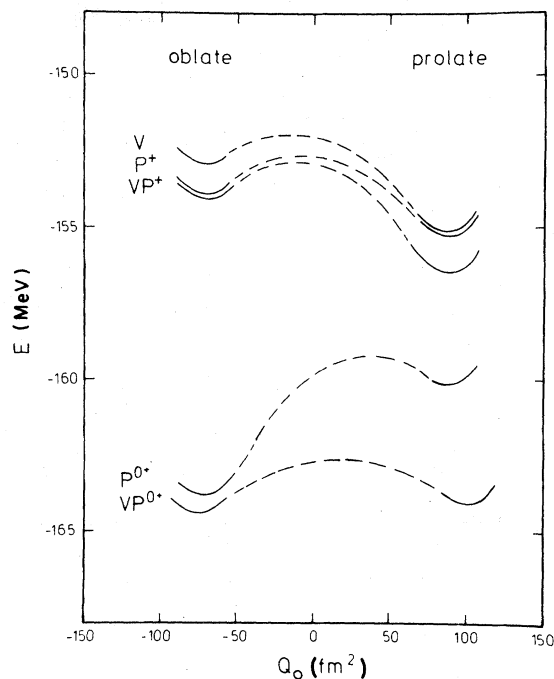


FIG. 1. Calculated oblate and prolate minima in ^{28}Si and the energy shifts resulting from variation before and after parity and angular momentum projection for the B_1 force. The approximations are labeled as in the text. The prolate and oblate minimum of each approximation are connected by arbitrary curves.

late states, and the resulting minima are almost degenerate.

We have studied the same approximations for all Brink-Boeker (B_1, \dots, B_4 , C_1, \dots, C_4) and Volkov (V_1, \dots, V_8) forces. Figure 2 shows the energy shifts resulting from each approximation for the different forces in the oblate [Fig. 2(a)] and prolate [Fig. 2(b)] state. Apart from sizable fluctuations in the oblate parity projection results P^+ and VP^+ , the energy shifts of the various approximations do not depend very sensitively on the particular choice of the interaction, and are qualitatively similar to the B_1 results of Fig. 1. In particular, the combined effect of parity and angular momentum projection, $P^{0+}V$ and VP^{0+} , falls, for all 16 forces, within 20% of the average value. Correspondingly, the shift in the excitation energy of the prolate minimum over the oblate minimum due to the $P^{0+}V$ and VP^{0+} approximation depends very little on the particular force. This is plotted in Fig. 3. The curves resulting from the projection ($P^{0+}V$) and the variation after projection (VP^{0+}) are almost parallel to the intrinsic result (V) for all forces. This demonstrates that the finding for the B_1 force in Fig. 1 is typical for all forces: While angular-momentum projection

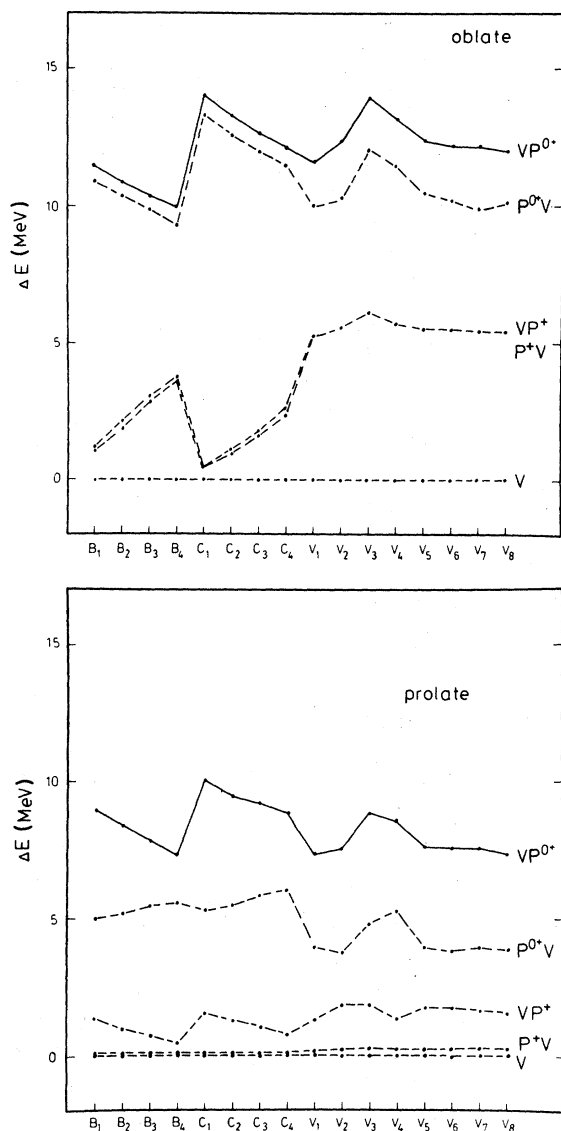


FIG. 2. Energy shifts resulting from parity and angular momentum projection before and after variation in the oblate [Fig. 2(a)] and prolate [Fig. 2(b)] cases for a number of nucleon-nucleon interactions. The approximations are labeled as in Fig. 1.

alone leads to a substantial improvement, much of the improvement is lost again in the full variation after projection. The remaining energy shift in the excitation of the prolate minimum due to variation after angular momentum projection is 2.5 to 5.1 MeV relative to the excitation calculated for the intrinsic states which is in most cases not sufficient to raise it above the oblate minimum. The only force that leads to a result in the vicinity of the experimental level spacing of 6.691 MeV is the C_1 force,

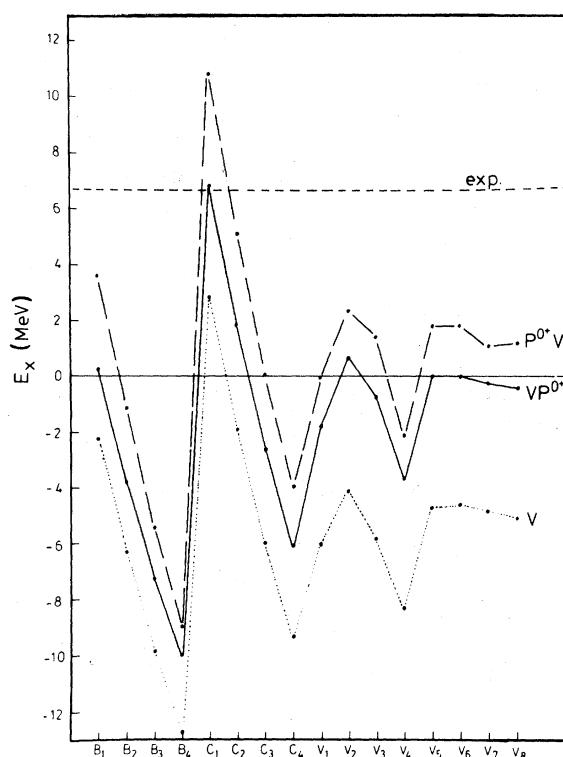


FIG. 3. Calculated excitation energy of the prolate minimum over the oblate minimum in ^{28}Si that result from variation without projection (V), and variation before ($P^{0+}V$) and after (VP^{0+}) projection onto $J^\pi=0^+$, $K=0$ for the Brink-Boeker and Volkov forces.

the only one that has already an oblate intrinsic ground state. The Brink-Boeker forces have an increasing strength of the odd state force within the B_1 to B_4 and C_1 to C_4 sets. The prolate-oblate splitting seems to be correlated to this strength leading to the zig-zag pattern of Fig. 3. No simple relation exists, however, for the energy shift if the sets B_i and C_i are compared with one another.

The total binding energy of the lowest calculated 0^+ state in ^{28}Si is given in Fig. 4. As in many nuclear structure calculations in the sd shell, the Brink-Boeker forces lead to a substantial underbinding whereas the Volkov forces are close to the experimental value⁴⁴ or tend to overbind.

The experimental data for ^{28}Si indicate that both the oblate and prolate band are rotational (Refs. 32, 33, 41, and 42). We have therefore determined the rotational constants $(E^{J^+} - E^{0^+})/J(J+1)$ that follow from the $J^\pi=2^+$ projection of the state of minimum 0^+ energy. The energy differences, $E^{2^+} - E^{0^+}$, are given in Fig. 5. The calculated rotational constants, again, do not depend very sensi-

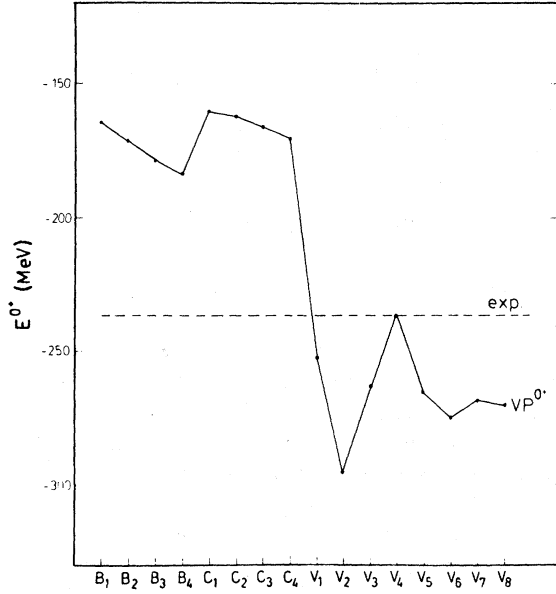


FIG. 4. The energy of the lowest calculated 0^+ state in ^{28}Si for the Brink-Boeker and Volkov forces. For comparison the experimental binding energy (Ref. 44) is also given.

tively on the choice of the nucleon-nucleon interaction. All our calculations slightly overestimate the experimental spacing of the prolate band, and underestimate the oblate spacing by a factor of 2 in accordance with most other calculations. In both bands the spacing may be further reduced in a variation of the 2^+ states after projection.

B. Angular momentum of the intrinsic states

For the rotational band with axial symmetry (i.e., only $K=0$) the energy shift due to angular-momentum projection (i.e., between the P^+V and the P^0+V energy) can be estimated on the basis of the intrinsic state $|\Phi\rangle$ and the experimental rotational constant.⁵ An expansion of $|\Phi\rangle$ in terms of angular momentum states $|\Phi_{0M}^J\rangle$ yields

$$\begin{aligned} E - E_{00}^0 &= \langle \Phi | H | \Phi \rangle - E_{00}^0 \\ &= \sum_{J \neq 0, M} |a_{0M}^J|^2 (E_{0M}^J - E_{00}^0), \end{aligned} \quad (3.1)$$

and the assumption of a rotational level spacing

$$E_{0M}^J - E_{00}^0 = \alpha J(J+1) \quad (3.2)$$

then leads to

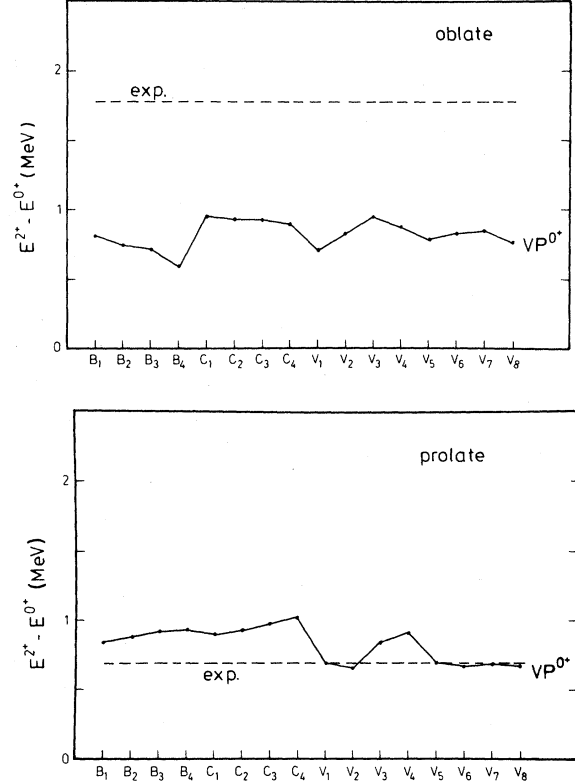


FIG. 5. Calculated energy differences $E^{2+} - E^{0+}$ for the oblate [Fig. 5(a)] and prolate [Fig. 5(b)] band in ^{28}Si in comparison with the experimental values. Here the 0^+ energy is the variation-after-projection result, whereas the 2^+ energy is determined by projecting the result of the variation after 0^+ projection onto 2^+ without further variation.

$$\begin{aligned} E - E_{00}^0 &= \alpha \sum_{J \neq 0, M} |a_{0M}^J|^2 J(J+1) \\ &= \alpha \langle \Phi | J^2 | \Phi \rangle, \end{aligned} \quad (3.3)$$

i.e., the energy shift $E - E_{00}^0$ should be small if the intrinsic state has little admixture of $J > 0$ components and therefore $\langle \Phi | J^2 | \Phi \rangle \approx 0$ and vice versa. This qualitative statement should also be valid if the intrinsic state is triaxial, but admixtures with $K \neq 0$ are small. This is the case in ^{28}Si where the next allowed K values are $K=6$ (prolate) and $K=10$ (oblate).

The calculated values of $\langle \Phi | J^2 | \Phi \rangle$ are given in Fig. 6 for the intrinsic prolate and oblate minimum energy states. The figure indicates that the oblate energy shift should be larger than the prolate one, provided that the rotational constants α are of the same order in both cases.

Following Ref. 5, a more quantitative estimate

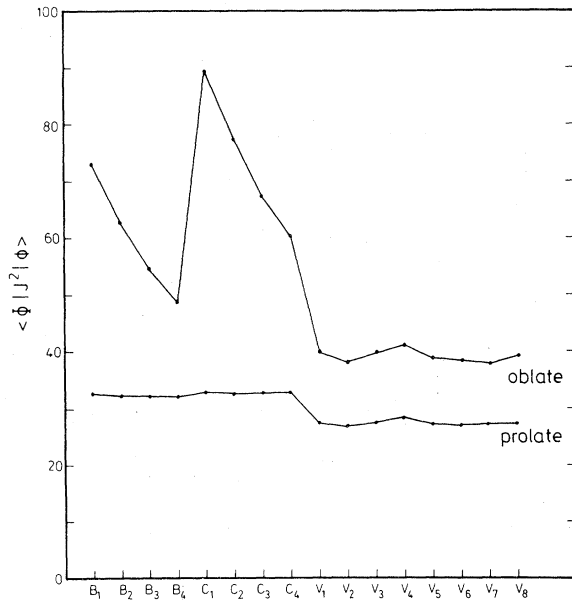


FIG. 6. Expectation value of the angular momentum J^2 in the intrinsic minimum energy state $|\Phi\rangle$. Large values of $\langle \Phi | J^2 | \Phi \rangle$ should be associated with large energy shifts in the 0^+ projection, as discussed in the text.

should be obtained by substituting the corresponding experimental values for α . A comparison with the exact results (i.e., the energy shift between the $P^{0+}V$ and P^+V calculations) is given in Fig. 7. While the approximation reproduces the force-dependent variations in the exact curves, and the or-

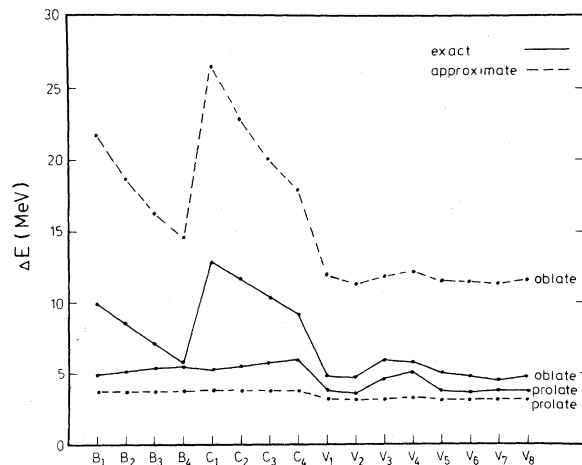


FIG. 7. Estimated and exact energy shifts $E^{0^+} - E^+$ due to angular momentum projection of the prolate and oblate intrinsic minimum energy state. Following Ref. 5, the estimate is based on the calculated intrinsic $\langle \Phi | J^2 | \Phi \rangle$ values of Fig. 6 and the experimental rotational constants of the prolate and oblate band.

der of magnitude in the prolate case, the oblate energy shift is generally overestimated by a factor of 2. This corresponds to the discrepancies in the calculated rotational constants that have been discussed in Sec. III A.

C. Deformations and densities

Figures 8 and 9 show the calculated rms radii and quadrupole moments. Generally the prolate and oblate state have similar rms radii (see Fig. 8). For all forces the projections onto good parity and angular momentum and the variations after the projections leave the rms radius of the intrinsic calculation almost unchanged. It turns out that the experimental charge radius of the ground state,^{17,43} $R_{\text{rms}} = 3.09$ to 3.13 fm, is better approximated by the Brink-Boeker forces than by the Volkov forces, whereas the opposite is valid for the binding energies. Similar results have been found in many other calculations.

The calculated quadrupole moments (Fig. 9) are also quite insensitive to the various approximation methods but much depend on the choice of the interaction. While the experimental quadrupole moment of the oblate state^{33,39,40} is approximated about equally well by the Brink-Boeker and the Volkov forces, the latter substantially underestimate the measured quadrupole moment of the prolate state.^{33,42}

Figure 10 shows the calculated single-particle densities

$$\rho(\vec{r}) = \langle \Phi | \sum_{i=1}^A \delta(\vec{r} - \vec{x}_i) | \Phi \rangle \quad (3.4)$$

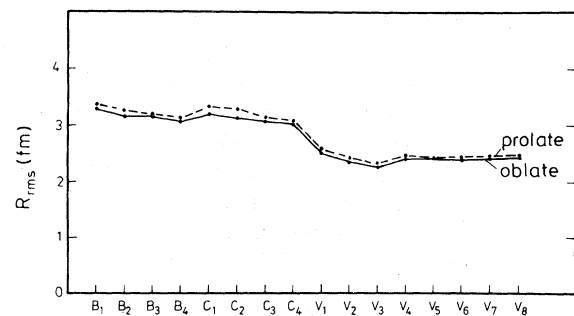


FIG. 8. Calculated rms radii of the prolate and oblate minimum in ^{28}Si for the Brink-Boeker and Volkov forces. Each radius corresponds to the VP^{0^+} expectation value for the intrinsic state which minimizes the energy after 0^+ projection. The results of the other approximations almost coincide with the plotted values. Experimental values (Refs. 17 and 43) for the charge rms radius of the oblate ground state are close to 3.1 fm.

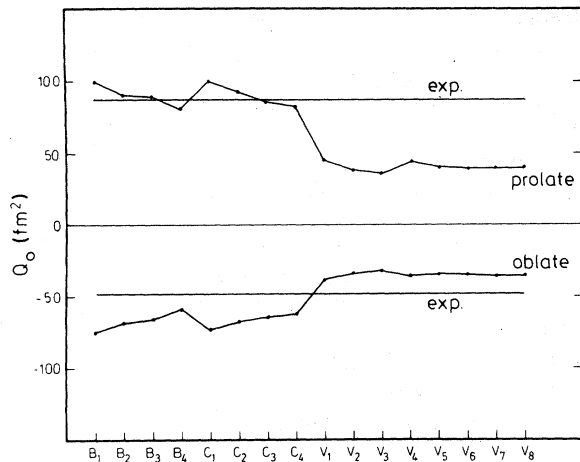


FIG. 9. Same as Fig. 8 for the quadrupole moments. The experimental values are taken from Refs. 33, 39, 40, and 42.

of the prolate and oblate intrinsic state perpendicular to the symmetry axis. It is obvious that the oblate state has much more azimuthal structure than the prolate one. This may qualitatively explain why the oblate state is more affected by rotations, and thus by angular momentum projection, than the prolate state.

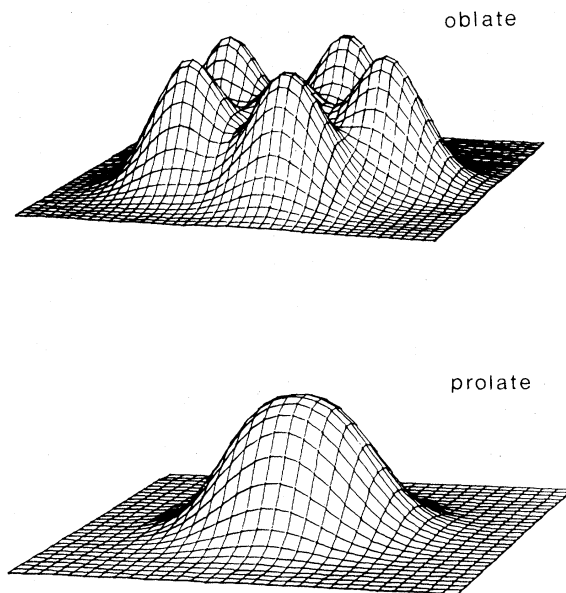


FIG. 10. Single particle density of the prolate and oblate minimum in ^{28}Si for the unprojected states and the B_1 interaction. Both plots are for a cut perpendicular to the axis of maximum symmetry of the wave function.

IV. CONCLUSIONS

According to this paper two minima with quadrupole moments of opposite sign coexist in ^{28}Si . This is the outcome of all calculations for all nucleon-nucleon forces studied, and in any approximation used. Apart from its very existence, the problem of prolate versus oblate deformation of the calculated ground state of ^{28}Si is ambiguous in two respects. Which one of the two local minima is lower in energy depends rather sensitively on the choice of the interaction, and on the treatment of parity and angular momentum projection and variation. In contrast to the experimental data most calculations tend to favor a prolate ground-state deformation. This is true for all unprojected results except for the C_1 force, and for 12 (two are degenerate) out of 16 results obtained by variation after projection. The C_1 interaction is the only one that results in a sizable excitation (6.8 MeV) of the prolate minimum over the oblate minimum. Therefore only the C_1 result is reasonably close to the measured excitation of the prolate 0^+ state in ^{28}Si (at 6.6914 MeV).

In general, projection after variation substantially lowers the energy of the oblate state, and therefore tends to decrease the discrepancy between experiment and calculation that usually results from unprojected calculations. However, by a further refinement of the approximation, viz., variation of the projected state, much of the improvement is lost again, and the disagreement between calculated and experimental deformation increases.

This may also be relevant for the existing Hartree-Fock results. For the B_1 force it has been shown in Ref. 30 that alpha-cluster model and Hartree-Fock calculations lead to rather similar states in ^{28}Si . Therefore much of the ambiguity associated with the projection will apply to Hartree-Fock results as well. In particular, there are a number of Hartree-Fock calculations with variation *before* projection only, which reproduce the sign of the experimental deformation. As the present results for ^{28}Si indicate, this may be at variance with the inclusion of the projection before variation, and no definite conclusion about the agreement between theory and experiment can be drawn unless the time-consuming variation *after* angular momentum projection has been performed.

This work was supported by the Deutsche Forschungsgemeinschaft.

- ¹S. Das Gupta and M. Harvey, Nucl. Phys. A94, 602 (1967).
- ²K. W. Schmid, L. Satpathy, and A. Faessler, Z. Phys. 267, 345 (1967).
- ³M. K. Pal and A. P. Stamp, Phys. Rev. 158, 924 (1967).
- ⁴R. Muthukrishnan, Nucl. Phys. A93, 417 (1967).
- ⁵P. U. Sauer, A. Faessler, H. H. Wolter, and M. M. Stingl, Nucl. Phys. A125, 257 (1969).
- ⁶B. Castel and J. P. Svenne, Nucl. Phys. A127, 141 (1969).
- ⁷Y. Abgrall, G. Baron, E. Caurier, and G. Monsonogo, Nucl. Phys. A131, 609 (1969).
- ⁸M. I. Friedman, Nucl. Phys. A159, 422 (1970).
- ⁹B. Castel and J. C. Parikh, Phys. Rev. C 1, 990 (1970).
- ¹⁰W. F. Ford, R. C. Braley, and J. Bar-Touv, Phys. Rev. C 4, 2099 (1971).
- ¹¹K. R. Lassey and A. B. Volkov, Phys. Lett. 36B, 4 (1971).
- ¹²J. Zofka and G. Ripka, Nucl. Phys. A168, 65 (1971).
- ¹³R. A. Nisley and M. H. Hull, Nucl. Phys. A198, 561 (1972).
- ¹⁴E. Elbaz *et al.*, Phys. Rev. C 7, 1445 (1973).
- ¹⁵S. P. Pandya and D. R. Kulkarni, *Proceedings of the International Conference on Nuclear Physics, Munich, 1973*, edited by J. de Boer and H. J. Mang (North-Holland, Amsterdam, 1973), Vol. 1, p. 46.
- ¹⁶P. Mpanias and M. L. Rustgi, Phys. Rev. C 9, 2261 (1974).
- ¹⁷C. Titin-Schnaider and Ph. Quentin, Phys. Lett. 49B, 213 (1974).
- ¹⁸A. L. Goodman, G. L. Struble, J. Bar-Touv, and A. Goswami, Phys. Rev. C 2, 380 (1970).
- ¹⁹M. R. Gunye, C. S. Warke, and S. B. Khadkikar, Phys. Rev. C 3, 1936 (1971).
- ²⁰M. Soyeur and A. P. Zuker, Phys. Lett. 41B, 135 (1972).
- ²¹S. S. M. Wong and G. D. Lougheed, Nucl. Phys. A295, 289 (1978).
- ²²J. P. Bernier and M. Harvey, Nucl. Phys. A94, 593 (1967).
- ²³M. Conze and P. Manakos, Phys. Lett. 69B, 29 (1977).
- ²⁴G. Leander and S. E. Larsson, Nucl. Phys. A239, 93 (1975).
- ²⁵I. Ragnarsson, S. Aberg, and R. K. Sheline, Lund Institute of Technology, Report Lund-M Ph-80/19, 1980.
- ²⁶S. B. Khadkikar and D. R. Kulkarni, Phys. Rev. C 10, 1189 (1974).
- ²⁷J. Pelet and J. Letourneux, Nucl. Phys. A281, 277 (1977).
- ²⁸D. M. Brink, H. Friedrich, A. Weiguny, and C. W. Wong, Phys. Lett. 33B, 143 (1970).
- ²⁹H. Schultheis and R. Schultheis, Phys. Rev. C 22, 1588 (1980).
- ³⁰W. Bauhoff, H. Schultheis, and R. Schultheis, Phys. Lett. 106B, 280 (1981).
- ³¹W. Bauhoff, H. Schultheis, and R. Schultheis, Phys. Lett. 110B, 92 (1982).
- ³²P. M. Endt and C. van der Leun, Nucl. Phys. A310, 1 (1978).
- ³³F. Glatz, P. Betz, J. Siefert, F. Heidinger, and H. Röpke, Phys. Rev. Lett. 46, 1559 (1981).
- ³⁴D. M. Brink and E. Boeker, Nucl. Phys. A91, 1 (1967).
- ³⁵D. M. Brink, in *Many-Body Description of Nuclear Structure and Reactions*, International School of Physics "Enrico Fermi", Course XXXVI, edited by C. Bloch (Academic, New York, 1966), p. 247.
- ³⁶A. B. Volkov, Nucl. Phys. 74, 33 (1965).
- ³⁷A. Arima, H. Horiuchi, K. Kubodera, and N. Takigawa, in *Advances in Nuclear Physics*, edited by M. Baranger and E. Vogt (Plenum, New York, 1972), Vol. 5, p. 345.
- ³⁸W. Bauhoff, H. Schultheis, and R. Schultheis, Phys. Lett. 95B, 5 (1980).
- ³⁹H. Rebel *et al.*, Nucl. Phys. A182, 145 (1972).
- ⁴⁰R. H. Spear, Phys. Rep. 73, 369 (1981).
- ⁴¹J. L. C. Ford *et al.*, Phys. Rev. C 21, 764 (1980).
- ⁴²F. Glatz *et al.*, Z. Phys. A 303, 239 (1981).
- ⁴³K. R. Lassey, M. R. P. Manning, and A. B. Volkov, Can. J. Phys. 51, 2522 (1973), and references therein.
- ⁴⁴J. H. E. Mattauch, W. Thiele, and A. H. Wapstra, Nucl. Phys. 67, 1 (1965).